Korean J. of Chem. Eng., **5**(2) (1988) *170-176*

THERMAL INSTABILITY OF PLANE POISEUILLE FLOW IN THE THERMAL ENTRANCE REGION

Dong June AHN and Chang Kyun CHOI

Department of Chemical Engineering, College of Engineering,
Seoul National University, Seoul 151-742, Korea

(Received 1 December 1987 • accepted 14 March 1988)

Abstract—The onset of thermal convection in plane Poiseuille flow is investigated theoretically. New stability equations are derived by using the propagation theory considering the variations of disturbance amplitudes in the main flow direction. In the thermal entrance region an analytical procedure to predict the critical conditions for extremely small Prandtl-number fluids is described, based on the local similarity. For $x_c \leq 0.01$ the critical Rayleigh numbers are well represented in the whole domain of the Prandtl number by

$$Ra_c = 200(1 + 0.123Pr^{-1})x_c^{-1}$$

under the conventional boundary layer theory. It is of much interest that the time-independent, three dimensional disturbances become more stable with a decrease in the Prandtl number.

INTRODUCTION

When a horizontal fluid layer is heated from below, buoyancy-driven convection occurs at high heating rates. In order to make an accurate heat transfer prediction it is necessary to examine the stability of a fluid layer. Furthermore the onset conditions of natural convection may be deeply interrelated with turbulent thermal convection, as was indicated by Howard[1]. The occurrence of longitudinal vortex rolls in plane Poiseuille flow due to buoyant force has been observed by several investigators[2-8].

The instability problem in the thermal entrance region for plane Poiseuille flow of a Newtonian fluid layer heated isothermally from below was analysed first by Hwang and Cheng[9]. In their analysis the disturbance amplitudes were assumed to be independent of the main flow direction. Their predictions on the critical Rayleigh number marking the onset of thermal convection were two orders of magnitude lower than the existing experimental data of water and air [3-5,8]. Yeo and Choi[10] analysed this problem by assuming the bottling effect of temperature disturbances confined within the thermal boundary layer. For large Prandtl numbers their analytical predictions were close to experimental data.

Very recently Kim and Choi[11] reformulated the stability equations by using the propagation theory introduced by Choi et al.[12], wherein the variations of disturbances in the main flow direction are considered. The two predictions of Yeo and Choi[10] and Kim and Choi[11] for large Prandtl number fluids were almost the same. Ahn and Choi[8] complemented the results of Kim and Choi[11] by producing the critical conditions for cases of extremely small Prandtl numbers. They neglected the disturbance of a velocity component in the main flow direction. Their results show that the critical Rayleigh number increases with a decrease in the Prandtl number, on the contrary to those of Hwang and Cheng[9].

The purpose of this present study is to extend the work of Ahn and Choi[8] by generating the new stability equations implying Prandtl's boundary layer concept and producing the related critical conditions. The analytical illustration will be limitted to the systems of extremely small Prandtl numbers.

THEORETICAL ANALYSIS

1. Base Temperature

The system considered here is the thermal entrance region of a Newtonian fluid confined between two horizontal infinite plates as shown in Fig. 1. The fluid temperature is uniform at T_1 for $X<0$ and there is a step change in the bottom temperature to a higher value T_2 at the position $X = 0$. The fluid properties are assumed constant and the viscous dissipation of energy is neglected. The velocity field is fully developed in the form of plane Poiseuille flow. We take the layer depth d as the unit of length, the temperature difference (T_2-T_1) as the unit of base temperature and the mean velocity U_m as the unit of base velocity. Then the

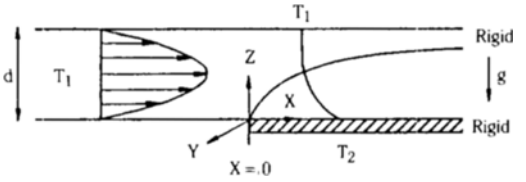

Fig. 1. Schematic diagram of system.

dimensionless base temperature profile can be obtained for pure forced convection by neglecting the axial heat conduction, as usual[10,13]:

$$u_o \frac{\partial \theta_o}{\partial x} = \frac{\partial^2 \theta_o}{\partial z^2} \tag{1}$$

where $x = X/(dPe)$ and $z = Z/d$. The boundary conditions are

$$\theta_o(0, z) = \theta_o(x, 1) = \theta_o(x, 0) - 1 = 0 \tag{2}$$

The exact solution brings mathematical difficulty in the stability analysis. Therefore we simplify the base temperature profile by using the integral method[14]:

$$\theta_o = (1 - \frac{3}{2}\zeta + \frac{1}{2}\zeta^3)(1 - H_{\zeta-1}) \tag{3}$$

where $\zeta = z/\delta_T$. H is a unit step function and δ_T is the dimensionless thermal boundary layer thickness having the value of $(\frac{15}{4}x)^{1/3}$. This approximate solution is in good agreement with the exact one in the region of $x \leq 0.01$. Since we are primarily concerned with the region of $\delta_T \ll 1$, the base velocity profile is approximated as follows:

$$u_o = 6\delta_T \zeta \tag{4}$$

The above approximation is based on the relation of $\delta_T \gg \delta_T^2$. Now we will see how the above approximate solutions (3) and (4) contribute to the stability analysis.

2. Formulation of Amplitude Equations

In the thermal entrance region of $\delta_T \ll 1$ the infinitesimal perturbations are superimposed on the base velocity, temperature and pressure fields. Using the linear stability theory under the Boussinesq approximation, we obtain the following time-independent neutral disturbance equations in dimensionless form:

$$\frac{1}{Pr}(u_o \frac{\partial u_1}{\partial x} + w_1 \frac{\partial u_o}{\partial z}) = \nabla^2 u_1 - \frac{1}{Pe^2}\frac{\partial p_1}{\partial x} \tag{5}$$

$$\frac{1}{Pr}(u_o \nabla^2 \frac{\partial w_1}{\partial x} - \frac{\partial w_1}{\partial x}\frac{\partial^2 u_o}{\partial z^2}) = \nabla^2 \nabla^2 w_1 + \frac{1}{Pe^2}\frac{\partial^2 \theta_1}{\partial x^2} + \frac{\partial^2 \theta_1}{\partial y^2} \tag{6}$$

$$u_o \frac{\partial \theta_1}{\partial x} + Ra(u_1 \frac{\partial \theta_o}{\partial x} + w_1 \frac{\partial \theta_o}{\partial z}) = \nabla^2 \theta_1 \tag{7}$$

where $\nabla^2(\cdot) = \frac{1}{Pe^2}\frac{\partial^2(\cdot)}{\partial x^2} + \frac{\partial^2(\cdot)}{\partial y^2} + \frac{\partial^2(\cdot)}{\partial z^2}$ Pr denotes the Prandtl number and Ra the Rayleigh number. It should be noted that the temperature disturbance, T′ is non-dimensionalized by $\theta_1 = RaT'/\Delta T$, which is different from other works [9-12, 15]. By invoking the conventional boundary layer theory, all the terms involving $1/Pe^2$ are neglected in equations (5) to (7). The pressure term in equation (5) disappears, which means that the pressure gradient in the main flow direction is maintained at the value of basic state around the onset. Accordingly, the second term in the left-hand side of equation (6) is neglected. Hwang and Cheng[9] neglected all the disturbance terms involving the x-derivatives and Ahn and Choi[8] set u_1 to zero. Therefore the present disturbance equations are completely different from the previous ones.

Now a new set of dimensionless variables is defined by using the vertical length scale of the dimensionless thermal boundary layer thickness δ_T:

$$\begin{pmatrix} u_1 \\ v_1 \\ w_1 \\ \theta_1 \end{pmatrix} = \begin{pmatrix} \delta_T^4 u^*(\zeta) \\ \delta_T^2 v^*(\zeta) \\ \delta_T^2 w^*(\zeta) \\ \theta^*(\zeta) \end{pmatrix} \cdot \exp(iay) \tag{8}$$

where the superscript '*' refers to the transformed amplitude of each disturbance term and 'a' indicates the dimensionless wave number meaning the transverse periodicity of disturbances. Substituting equations (4) and (8) into the resulting disturbance equations (5) to (7), we can generate the new amplitude equations:

$$\frac{1}{Pr}(-\frac{15}{2}(\zeta^2 D - 4\zeta)u^* + 6w^*) - (D^2 - a^{*2})u^* \tag{9}$$

$$\frac{1}{Pr}(-\frac{15}{2}(\zeta^2 D^3 - a^{*2}\zeta^2 D + 2a^{*2}\zeta)w^*) = (D^2 - a^{*2})w^* - a^{*2}\theta^* \tag{10}$$

$$-\frac{15}{2}\zeta^2 D\theta^* + Ra^*(-\frac{5}{4}\zeta u^* + w^*)D\theta_o = (D^2 - a^{*2})\theta^* \tag{11}$$

where $D(\cdot) = d(\cdot)/d\zeta$, $a^* = a\delta_T$ and $Ra^* = Ra\delta_T^3$. Experimental evidences have shown that the new parameters a^* and Ra^* having the vertical length scale of δ_T would be kept constant for $x \leq 0.1$[3-5]. Up to this point the related concepts represent the essence of the propagation theory. It is surprising that the concept of local similarity is realized in this procedure.

For the limiting case of $Pr \to \infty$ the stability criteria were reported by Kim and Choi[11]. It is noted that their stability equations involving the effect of the Prandtl number are not quite general. But their stability criteria are exactly the same as those based on equa-

tions (9) to (11) since u_1 disappears for the infinite Prandtl number case. Therefore we proceed to analyse the instability for the limiting case of $Pr \to 0$. As the Prandtl number decreases, the convective terms related with u^* and w^* in equations (9) to (10) become important. Then in the case of $Pr \to 0$ the stability equations can be formulated as

$$\frac{15}{2} F(D) u_i^* = a^{*2} PrRa^* D\theta_o (\zeta^2 D - 5\zeta) u_i^* \quad \text{for } 0 \leqq \zeta < 1 \tag{12}$$

$$F(D) u_o^* = 0 \quad \text{for } \zeta \geqq 1 \tag{13}$$

where

$$F(D) = (D^2 + \frac{15}{2}\zeta^2 D - a^{*2})(\zeta^2 D^3 - a^{*2}\zeta^2 D + 2a^{*2}\zeta)(\zeta^2 D - 4\zeta) \tag{14}$$

The subscripts 'i' and 'o' refer to the inner and the outer region of the thermal boundary layer, respectively.

The proper boundary conditions are constructed as

$$w^* = \theta^* = 0 \quad \text{at } \zeta = 0 \tag{15}$$

$$u_i^*, w_i^*, \theta_i^*, DW^* \to 0 \quad \text{as } \zeta \to \infty \tag{16}$$

These conditions satisfy those of flat surfaces with constant temperature. Since a slip condition should be applied to the case of $Pr \to 0$, the conditions of $u^* = Dw^* = 0$ at the bottom rigid boundary are relaxed. The corresponding boundary conditions in terms of u^* are produced from equations (9) and (10). The interface conditions at $\zeta = 1$ are constructed by considering equations (12) to (13):

$$D^n u_i^* - D^n u_o^* = 0 \; ; \; n = 0, 1, 2, 3, 4, 5 \tag{17}$$

Now the problem is to find the minimum value of $PrRa^*$ and its corresponding wave number to satisfy all the above equations (12) to (17). These values are the critical conditions marking the onset of natural convection in the form of longitudinal vortex rolls.

SOLUTION PROCEDURE

The solution of the inner region of thermal boundary layer is found by the Frobenius method as follows:

$$u_i^* = \sum_{j=1}^{6} C_j f_j(\zeta) \tag{18}$$

where $f_j(\zeta) = \sum_{n=0}^{\infty} B_n^j \zeta^n$. C_j is an arbitrary constant and B_n^j is obtained from the recursion formula generated from equation (12). By applying the boundary conditions (14), u_i^* is easily obtained:

$$u_i^* = C_2 f_2 + C_3 f_3 + C_4 f_4 + C_6 f_6 \tag{19}$$

where

$$f_2 = 1 - \frac{a^{*2}}{3}\zeta^2 - \frac{a^{*2}}{144} PrRa^* \zeta^3 - - - + + + \tag{20}$$

$$f_3 = \zeta - \frac{a^{*2}}{15750} PrRa^* \zeta^6 + - + - + - \tag{21}$$

$$f_4 = \zeta^4 + \frac{a^{*2}}{211680} PrRa^* \zeta^7 - - - + + + \tag{22}$$

$$f_6 = f_3 \ln\zeta + \frac{a^{*2}}{6}\zeta^3 - \frac{23a^{*4}}{7200}\zeta^5 + - + - + - \tag{23}$$

To obtain the solution of the outer region we divide equation (13) into two equations as follows:

$$(D^2 + \frac{15}{2}\zeta^2 D - a^{*2}) Y = 0 \tag{24}$$

$$\zeta(D^2 - a^{*2})(\zeta D - 2)\zeta(\zeta D - 4) u_o^* = Y \tag{25}$$

Equation (24) can be solved by employing the WKB method:

$$Y(\zeta) \simeq \exp\Big(-\frac{5}{4}\zeta^3 - \int_1^{\zeta} (\frac{225}{16}\eta^4 + \frac{15}{2}\eta + a^{*2})^{1/2} d\eta\Big) / (\frac{225}{16}\zeta^4 + \frac{15}{2}\zeta + a^{*2})^{1/4} \tag{26}$$

which satisfies the upper boundary condition of $\theta^* \to 0$ i.e., $Y \to 0$, as $\xi \to \infty$. By approximating this solution as the appropriate power-series forms, the solution of equation (25) can be found as follows:

$$u_o^* = C_7 f_7 + \frac{C_6}{2a^*}\Big\{e^{a^*(\zeta-1)} \sum_{k=0}^{\infty} Q_k (\zeta-1)^k + e^{-a^*(\zeta-1)} \sum_{k=0}^{\infty} R_k (\zeta-1)^k\Big\} \tag{27}$$

where

$$f_7 = (\zeta^{-1} - \frac{3}{2}a^* - \frac{a^{*2}}{18}\zeta + \frac{a^{*3}}{36}\zeta^2 - \frac{a^{*4}}{36}\zeta^3)\frac{e^{-a^*\zeta}}{10} + (\frac{a^{*2}}{6}\zeta + \frac{a^{*5}}{360}\zeta^4)\int_{\zeta}^{\infty} \frac{e^{-a^*\eta}}{\eta} d\eta \tag{28}$$

$f_7(\zeta)$ is the homogeneous solution of u_o^*. The coefficients Q_k and R_k can be easily obtained from the recursion formulae by following the procedure illustrated in the work of Yoo et al.[15], which are valid near $\zeta = 1$. The above solution satisfies the upper boundary conditions (16).

The remaining interface conditions (17) make it possible to generate the following secular equation:

$$\begin{vmatrix} f_2 & f_3 & f_4 & f_6 & f_7 & 0 \\ f_2^{(1)} & f_3^{(1)} & f_4^{(1)} & f_6^{(1)} & f_7^{(1)} & 0 \\ f_2^{(2)} & f_3^{(2)} & f_4^{(2)} & f_6^{(2)} & f_7^{(2)} & 0 \\ f_2^{(3)} & f_3^{(3)} & f_4^{(3)} & f_6^{(3)} & f_7^{(3)} & 0 \\ f_2^{(4)} & f_3^{(4)} & f_4^{(4)} & f_6^{(4)} & f_7^{(4)} & -Y(1) \\ f_2^{(5)} & f_3^{(5)} & f_4^{(5)} & f_6^{(5)} & f_7^{(5)} & 6Y(1) - Y^{(1)}(1) \end{vmatrix} = 0 \tag{29}$$

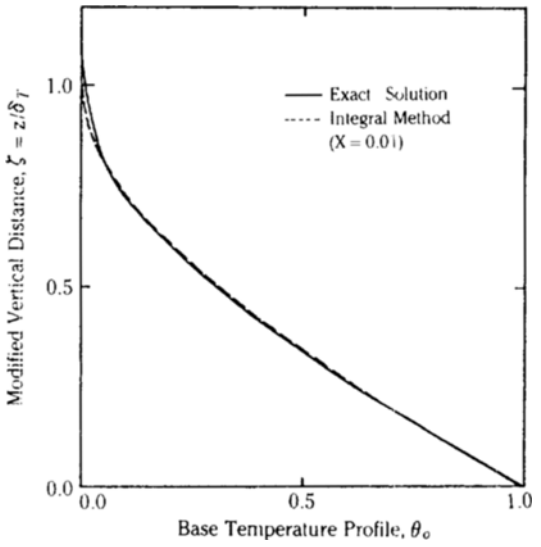

Fig. 2. Base temperature profile.

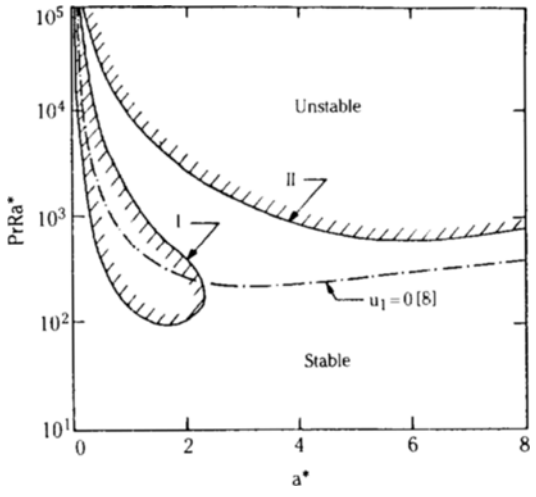

Fig. 3. Stability diagram.

where the superscript (n) indicates the order of differentiation with respect to ζ. Once eigenvalues of PrRa* and a* are found, we can construct the stability diagram and obtain u*. Then w* and θ^* can be computed by using equations (9) and (10), respectively. The spanwise velocity v* can be found from the equation of continuity as follows:

$$v^* = \left(\frac{5}{4}(\zeta D - 4)u^* - Dw^*\right)/a^* \tag{30}$$

RESULTS AND DISCUSSION

By involving the streamwise velocity disturbance u_1 with $\frac{\partial p_1}{\partial x} = 0$, the stability diagram is obtained in Fig. 3 according to the procedure outlined in the preceding section. The solid curves indicate the present results, while the dotted curve represents those of Ahn and Choi[8] for the case of $u_1 = 0$ and $\frac{\partial p_1}{\partial x} \neq 0$. The present critical conditions are found:

$$PrRa_c^* = 92.2 \quad \text{and} \quad a_c^* = 1.64 \quad \text{for} \quad Pr \to 0 \tag{31}$$

This means that for extremely small Pr and δ_T the secondary flow of natural convection may occur with the three component velocity field of u_1, v_1 and w_1 characterized by the conditions (31), independently of time. If we invoke the principle of exchange of stabilities as usual, the magnitudes of disturbances will be amplified with time in the hatched unstable region but it will be deamplified with time in the stable region. This principle excluding the possibility of wave instabilities has been used in most of thermal instability problems. For large Pr fluids this is justified by experimental evidences[2-8]. It is unfortunate that for extremely small Pr fluids its validity remains an unresolved problem.

Ahn and Choi[8] obtained the critical conditions of $PrRa_c^* = 212.1$ and $a_c^* = 3.14$ with $u_1 = 0$ and $\frac{\partial p_1}{\partial x} \neq 0$. These values are almost two times higher than those in equation (31). Therefore the existence of u_1 seems to make the system more unstable. This is justified by examining Fig. 4, which shows that at the critical condition two convective heat transport terms of velocity disturbances have the same sign. It appears evident that the term $u_1 \frac{\partial \theta_0}{\partial x}$ has the adverse effect on the stability in addition to the term $w_1 \frac{\partial \theta_0}{\partial x}$, on the contrary to the effect of the term $u_0 \frac{\partial \theta_1}{\partial z}$. The last term is already known to have the stabilizing effect[11,12,15].

In order to examine the disturbance fields the am-

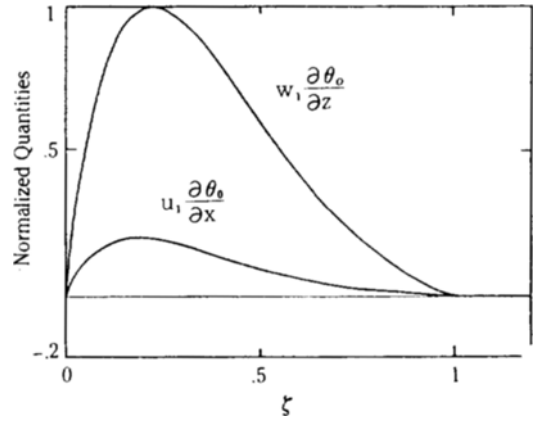

Fig. 4. Effect of convective terms of velocity disturbances at critical condition.

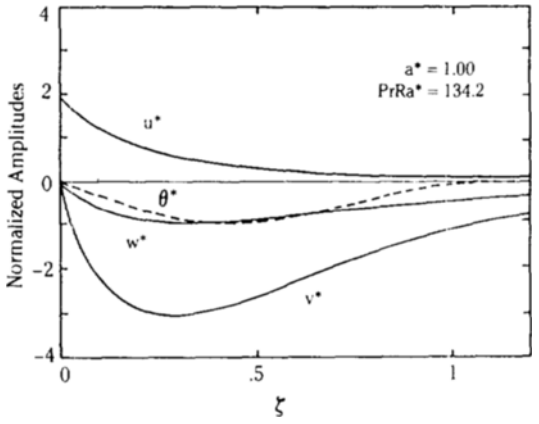

Fig. 5. Distribution of amplitudes of disturbances at PrRa* = 134.2 and a* = 1.00.

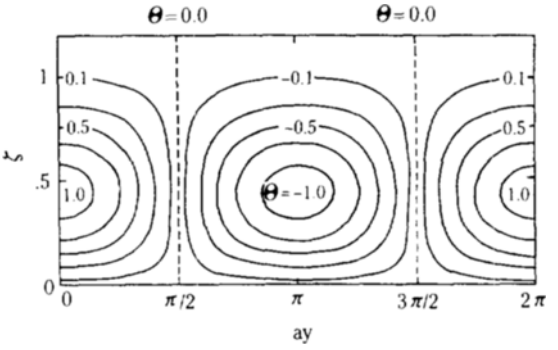

Fig. 7. Isotherms of disturbances at PrRa* = 134.2 and a* = 1.00.

plitude functions of velocity and temperature disturbances are normalized in terms of the maximum value of absolute magnitudes of w* and θ*, respectively. The normalized amplitudes, the streamlines and the isotherms of disturbances at two points placed on the neutral stability curve I are plotted in Figs. 5 to 10 in turn. Though the velocity field of disturbance is three dimensional, it is, however, possible to introduce the stream function based on the axisymmetry in a y-z plane for a fixed x. And the isotherms given here indicate the temperature fluctuation of the secondary flow. At the point of PrRa* = 134.2 and a* = 1.00 the velocity disturbances constitute semi-circular streamlines in the projected y-z plane and the temperature disturbance is mainly confined within the basic thermal boundary layer. These are illustrated in Figs. 5 to 7. The slip condition of u* at the bottom boundary gives birth to the streamwise velocity at $\zeta = 0$. The counterclockwise movement along the curve I is followed by the another cellular motion over the lower semi-circular motion due to the inversion of the temperature disturbance, as shown in Figs. 8 to 10. The latter motion becomes smaller and finally fades away during the successive advance. The neutral stability curve II generates the almost regular logitudinal vortex-type instabilities, as illustrated in Fig. 11. This

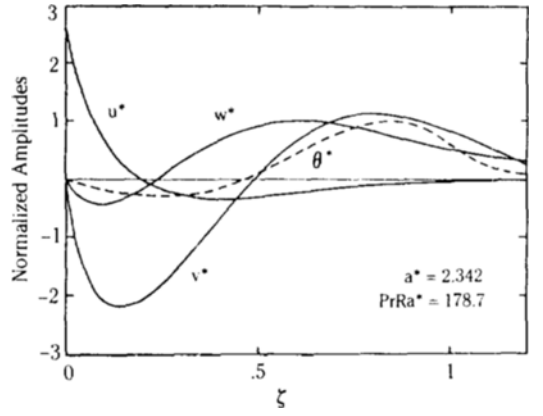

Fig. 8. Distribution of amplitudes of disturbances at PrRa* = 178.7 and a* = 2.34.

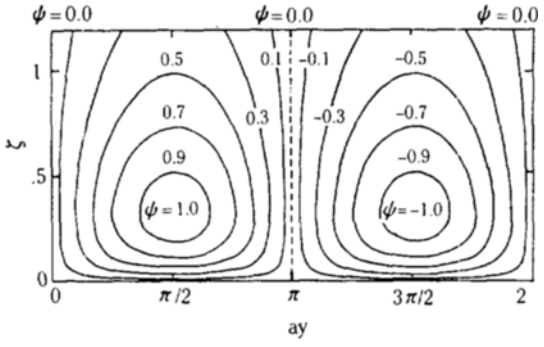

Fig. 6. Streamlines of disturbances at PrRa* = 134.2 and a* = 1.00.

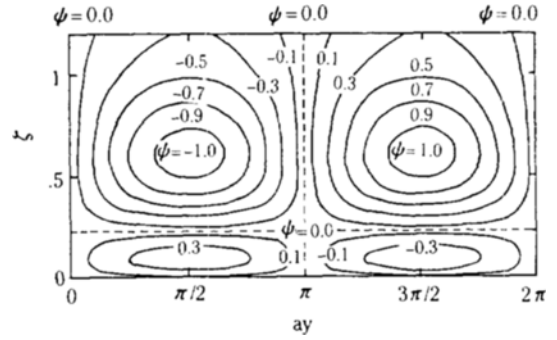

Fig. 9. Streamlines of disturbances at PrRa* = 178.7 and a* = 2.34.

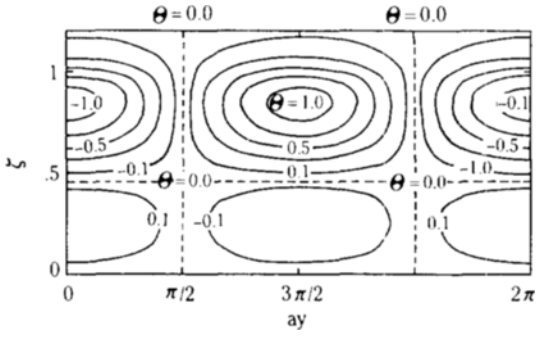

Fig. 10. Isotherms of disturbances at PrRa* = 178.7 and a* = 2.34.

figure represents those amplitudes for the minimum value of PrRa* on the curve II, and the disturbance patterns are similar to those in the work of Ahn and Choi[8]. Therefore it is expected that the distinction between the two inner curves will disappear at the high PrRa* region, wherein the lower semi-circular motion becomes negligible.

The above-mentioned trend is very peculiar in comparison with the conventional stability diagrams. The curve I is very similar to that of wave instability and the curve II to that of regular longitudinal vortex instability. It is well known that the latter-type stability diagram prevails at large Pr cases[9-12,15]. Therefore it may be stated that the resultant secondary motion becomes simplified with an increase in Pr, leading to the regular vortex roll. Meanwhile through these figures it is known that the magnitude of v* is inversely proportional to the wave number according to equation (30).

The conditions (31) marking the onset of natural convection for Pr→0 are of much interest, here. The disturbance amplitudes decay so sharply for $\zeta > 1$. It should be noted that the present critical values are

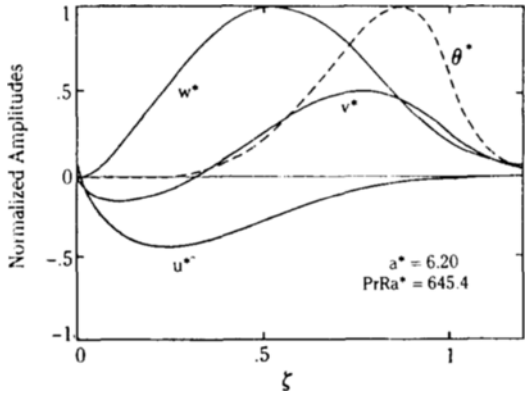

Fig. 11. Distribution of amplitudes of disturbances at PrRa* = 645.4 and a* = 6.20.

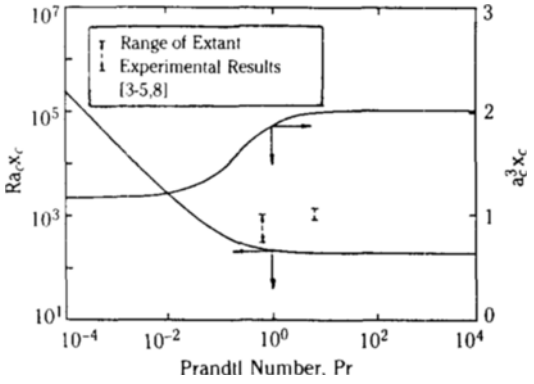

Fig. 12. Effect of Prandtl number on critical conditions.

valid if $\delta_T \ll 1$. By combining these values with the results of Kim and Choi[11] for Pr→∞, the critical conditions in the thermal entrance region may be represented in the whole domain of Pr as follows:

$$Ra_c x_c = 200\,(1+0.123/Pr) \tag{32}$$

$$a_c^3 x_c = 2.02\,[1-0.088/(Pr+0.211)] \tag{33}$$

These relationships are plotted in Fig. 12, which shows that the effect of the Prandtl number is almost negligible for Pr≥1. In this connection more refined work is now in progress in our laboratory.

The present analysis involves the term $u_o \frac{\partial \theta_1}{\partial x}$ to stabilize the flow. Hwang and Cheng[9] neglected this term and they reported that for Pe→∞ the critical Rayleigh number decreases with a decrease in Pr for a given x_c. It seems evident that their critical conditions are unreasonable, for the term $u_o \frac{\partial \theta_1}{\partial x}$ has the much stronger stabilizing effect in comparison with the destabilizing effect of the term $Ra\, u_1 \frac{\partial \theta_o}{\partial x}$ in equation (7). The experimental evidences are available only for air [3-5] and water[8]. The present analysis makes predictions close to experimental data as compared in Fig. 12. It is noted that the secondary motion of vortex-type convection will require a growth distance to manifest detection. The experimental study for small Prandtl number fluids is in great request. It is very interesting that the critical Rayleigh number predicted in this study is in good agreement with the experimental result given by Jorné and Labelle[16] for the electrochemical mass transfer system.

CONCLUSION

The onset of thermal instability in the thermal entrance region of plane Poiseuille flow has been examined by the propagation theory. For $x_c \leq 0.01$ the critical Rayleigh numbers are represented by

$Ra_c = 200(1 + 0.123Pr^{-1})x_c^{-1}$

under the conventional boundary layer theory. The present analysis introducing the three component velocity field of disturbance made predictions in close agreement with experimental data. It seems evident that the results of Hwang and Cheng[9] lose the validity.

ACKNOWLEDGEMENT

The authors deeply appreciate the financial support of the Korea Science and Engineering Foundation, Daeduck.

NOMENCLATURE

a : dimensionless wave number
a* : modified wave number [$=a\delta_T$]
d : depth of fluid layer (m)
g : gravitational acceleration (m/sec^2)
i : complex number
P : pressure (N/m^2)
p : dimensionless pressure [$=Pd^2/\alpha/\mu$]
Pe : Peclet number [=PrRe]
Pr : Prandtl number [$=\nu/\alpha$]
Ra : Rayleigh number [$=g\beta d^3\Delta T/\alpha/\nu$]
Ra* : modified Rayleigh number [$=Ra\delta_T^3$]
Re : Reynolds number [$=U_m d/\nu$]
T : temperature (K)
T_1 : temperature of inlet flow and upper rigid boundary (K)
T_2 : temperature of heated bottom plate (K)
ΔT : temperature difference between boundaries [$=T_2-T_1$] (K)
U, V, W : velocities in rectangular coordinates (m/sec)
U_m : mean basic flow velocity (m/sec)
u, v, w : dimensionless velocities [=(U/Pe, V, W) d/α]
u_o : dimensionless base flow velocity [$=U_b/U_m$]
X, Y, Z : positions in rectangular coordinates (m)
x, y, z : dimensionless position [=(X/Pe, Y, Z)/d]

Greek Letters

α : thermal diffusivity (m^2/sec)
β : thermal expansion coefficient ($1/K$)
Δ_T : thermal boundary layer thickness (m)
δ_T : dimensionless thermal boundary layer thickness [$=\Delta_T/d$]
ζ : similarity variable [$=z/\delta_T$]
θ : normalized isotherm of disturbance
θ_o : dimensionless base temperature [$=(T-T_1)/\Delta T$]
θ_1 : dimensionless temperature disturbance [$=RaT'/\Delta T$]
μ : viscosity (kg/m/sec)
ν : kinematic viscosity (m^2/sec)
ψ : normalized stream function of disturbance

Subscripts

b : base quantity
c : critical condition
i : inner region of thermal boundary layer
o : outer region of thermal boundary layer
0 : dimensionless base quantity
1 : dimensionless disturbance quantity

Superscripts

n,(n) : order of differentiation with respect to ζ in equations (17) and (29), respectively
* : amplitude function of disturbance
' : disturbance quantity

REFERENCES

1. Howard, L.N.: Proc. 11th Int. Congress Applied Mech., Munich, pp. 1109-1115 (1964).
2. Akiyama, M., Hwang, G.J. and Cheng, K.C.: *J. Heat Transfer,* **93,** 335 (1971).
3. Hwang, G.J. and Liu, C.L.: *Can. J. Chem. Eng.,* **54,** 521 (1976).
4. Kamotani, Y. and Ostrach, S.: *J. Heat Transfer,* **98,** 62 (1976).
5. Kamotani, Y., Ostrach, S. and Miao, H.: *J. Heat Transfer,* **101,** 222 (1979).
6. Maughan, J.R. and Incropera, F.P.: *Exp. Fluids,* **5,** 334 (1987).
7. Maughan, J.R. and Incropera, F.P.: *Int. J. Heat Mass Transfer,* **30,** 1307 (1987).
8. Ahn, D.J. and Choi, C.K.: *Hwahak Gonghak,* **25,** 614 (1987).
9. Hwang, G.J. and Cheng, K.C.: *J. Heat Transfer,* **95,** 72 (1973).
10. Yeo, Y.K. and Choi, C.K.: *Int. Chem. Eng.,* **23,** 281 (1983).
11. Kim, J.J. and Choi, C.K.: Proc. World Congress III of Chem. Eng., Tokyo, vol. 2, pp. 328-331 (1986).
12. Choi, C.K., Shin, C.B. and Hwang, S.T.: Proc. Int. Heat Transfer Conference, San Francisco, pp. 1389-1394 (1986).
13. Edwards, V. and Newman, J.: *Int. J. Heat Mass Transfer,* **28,** 503 (1985).
14. Das, R. and Mohanty, A.K.: *Int. J. Heat Mass Transfer,* **26,** 1403 (1983).
15. Yoo, J.Y., Park, P., Choi, C.K. and Ro, S.T.: *Int. J. Heat Mass Transfer,* **30,** 927 (1987).
16. Jorne, J. and Labelle, D.: *Chem. Eng. Commun.,* **38,** 347 (1985).